# Experimental Analysis of GPS L2C Signal Quality under Various Observational Conditions

**Yun, S.[1] and Lee, H.[2]***
[1]Department of Eco-Friendly Offshore Plant FEED Engineering, Changwon National University, Changwon, Republic of Korea, E-mail: shyun92@changwon.ac.kr
[2]Department of Civil Engineering, Changwon National University, Changwon, Republic of Korea, E-mail: hkyulee@changwon.ac.kr
*Corresponding Author*

**DOI: https://doi.org/10.52939/ijg.v18i3.2199**

**Abstract**
*To appropriately handle the GPS L2C signal for the future development of positioning algorithms, this contribution has endeavoured to figure out its features by computing some quality measures of all the modernised satellites (i.e., twenty-three as of January 2022) and comparing them with those of the C/A and P2(Y) code. A series of quality analyses have been carried out to GPS measurements at twenty-four continuously operating reference stations (CORS) equipped with eight receiver models. In addition, experimental data acquired by a combination of high-end and cost-effective receivers have been intensively assessed to characterise the relative signal quality of the L2C to the legacy codes. The observational conditions considered in this study include different multipath environments and receiver dynamics. The results of the analyses, in general, indicate that the quality of the L2C-derived measurements is equivalent to the legacy civilian code (i.e., C/A) but superior to the encrypted military signal (P2(Y)). Hence, it is expected that the new civilian GPS signal enhances the positioning performance of dual-frequency measurements with both high-end and cost-effective receivers.*

## 1. Introduction

The modernisation of the United States (US) global positioning system (GPS) has been underway since 2000 to improve signal availability, integrity and the accuracy of positioning and timing (Esper et al., 2020 and NOAA, 2021a). This modernisation is an ongoing effort to upgrade the GPS space and control segment. The essence of the space segment modernisation lies in the additional provision of new pseudo-random noise (PRN) codes, such as L1C and L2C and an additional L5 carrier-phase. Especially, L2C is the second civilian code provided by the Block IIR-M satellite placed in an orbit since 2005. As of January 2022, all 23 modernised space vehicles (SVs) transmit L2C signals (NAVCEN, 2022). To this end, civilian users of GPS single point positioning (SPP) with dual-frequency observations have an opportunity to improve the positioning accuracy via modelling the ionospheric delay. L2C enables GPS dual-frequency receivers to more robustly track L2 carrier-phase (Rizos et al., 2005). Since the transmission of legacy military signals P(Y) will be stopped according to the US Federal Radionavigation Plan (Esper et al., 2020), the importance of L2C in high-precision positioning is expected to increase further. Simsky et al., (2006) compared the signal-to-noise ratio (SNR) and magnitude of the multipath and noise of L2C signals of the first modernised SV (Block IIR-M model) acquired by the Septentrio PolaRx2C receiver with those of the coarse/acquisition (C/A) code and showed that the quality of these signals was generally equivalent. Sukeova et al., (2007) analysed the L2C signal quality using a method similar to Simsky et al., (2006). They analysed the data from Trimble NetRS, NetR5, and R7 receivers to examine the differences in signal quality between them. The results, in general, revealed that the multipath was similar to that between the C/A and L2C acquired by NetR5. In contrast, the multipath of L2C of NetRS was more severe than that of C/A as a mitigation algorithm was applied to only C/A in NetRS, unlike NetR5. This study also pointed out that the discrepancy in the multipath of C/A and L2C acquired by R7 would be attributed to the application/non-application of the mitigation algorithm.

al-Fanek et al., (2007) used a Novatel OEMV3 receiver to observe C/A, L2C, and P2(Y) signals emitted by three Block IIR-M SVs and analysed the signals by adding the phase acquisition rate to the signal quality metrics used in Simsky et al., (2006) and Sukeova et al., (2007). They showed that L2C's SNR and pseudo-range (PR) multipath are similar to C/A, whereas L2C has less noise than C/A because of limited cross-correlation interferences and the L2C tracking algorithm implemented on OEMV3. Furthermore, by reproducing a weak signal environment using an in-line attenuator and comparing the expected and actual number of acquired data, al-Fanek et al., (2007) presented that the actual quantity of acquired data for L2C and L1 C/A was slightly smaller than the expected number, but that of P2(Y) was 25% to 50% smaller. These three studies analysed the quality and features of L2C corresponding to the first modernised signals with legacy signals, but they had limitations; signals of one to three early-version Block IIR-M SVs - the first modernised satellite model - placed in orbits were acquired using geodetic grade receivers in the static mode under only benign observation environments.

To overcome the limitation of the pervious researches and further understand the characteristics of GPS L2C signal, which is crucial for stochastic modelling of the measurements, this study has made an attempt to comprehensively analyse the satellite signals and measurements. The L2C signals and observations transmitted by all GPS modernised SVs as of January 2022 for different receiver types and dynamics and operational environments were acquired. Their quality and features were then examined by comparing them with the legacy signals. The observational data used in the analysis were PR and carrier-phase (CPH) measurements of C/A, L2C, and P2(Y) signals, and quality measures used in the quality analysis include data acquisition rate, SNR, multipath, and noise. The remainder of this paper is organised as follows: Section 2 summarises the features of GPS L2C signals. Section 3 introduces the conditions and methods of acquiring GPS data used in the analysis and signal quality indicators. Section 4 presents and discusses the quality analysis results of the data acquired under various conditions. Finally, Section 5 summarises the features of L2C quality based on the analysis results.

## 2. Features of GPS L2C

Since the early 2000s, the US government has been continuously implementing a modernisation program to improve the overall performance of GPS by upgrading the space and control segments. The provision of new signals, L1C, L2C, and L5, is noteworthy in this program. Table 1 summarises the status of the SV constellation classified by blocks as of January 2022. L2C, the first modernised ranging signal, was transmitted by the Block IIR-M, launched in 2005. L5 is a new carrier-phase added for secure and robust positioning in safety-of-life fields, including aviation and transportation, and is started to be transmitted by the Block IIF. L1C is the third modernised signal designed for interoperability with other global navigation satellite systems (GNSS), such as Gailieo and BeiDou, and was given from Block III where four SVs have been currently deployed (NOAA, 2021b). According to Table 1, 23 modernised satellites out of 30 SVs are emitting L2C.

The characteristics of the L2C were compared to those of C/A and summarised in Table 2. L2C is modulated on the L2 band carrier. Unlike the C/A consisting of a single code, the modernised signal has a unique characteristic comprising two codes, civil moderate (CM) and civil long (CL). The CM code has a length of 10,230 chips and a chip rate of 511.5 kHz, and it is repeated every 20 ms, whereas the CL code has a length of 767,250 chips, the same chip rate as the CM code, and a repetition period of 1,500 ms (Fontana et al., 2001). Unlike the CL code, the CM code is modulated with a navigation message of 25 bps.

Table 1: Status of GPS satellite constellation in January 2022

| **Satellite model** | **Legacy** | **Modernisation** | | |
|---|---|---|---|---|
| **(Block)** | **IIR** | **IIR-M** | **IIF** | **III** |
| Transmitting Signals | C/A, P(Y) | All legacy signals + L2C | All IIR-M signals + L5 | All IIF signals + L1C |
| Number in orbit | 7 | 7 | 12 | 4 |

| Year of launch | 1997 - 2004 | 2005 - 2009 | 2010 - 2016 | 2018 - |
|---|---|---|---|---|

Table 2: General features of GPS ranging signals (Fontana et at., 2001 and Cho et al., 2004)

| **Signal (Band and Code)** | **L1 C/A** | **L2 CM** | **L2 CL** | **L2 CM & CL** |
|---|---|---|---|---|
| Frequency (MHz) | 1,575.42 | 1,227.60 | | |
| Chip rate (MHz) | 1.023 | 0.5115 | 0.5115 | 1.023 |
| Code length (chips) | 1,023 | 10,230 | 767,250 | 1,534,500 |
| Duration (msec) | 1 | 20 | 1,500 | 1,500 |
| Bit rate | 50 bps | 25 bps | No message | 50 bps |

Because the two codes are transmitted simultaneously via the so-called time-division multiplexing (TDM) technology, they can be used individually or together, depending on the application field (Grewal et al., 2020). When receivers track the CM and CL codes simultaneously, the chip rate is the same as that of C/A, and consequently, the PR multipath and the noise size are similar (Simsky et al., 2006, al-Fanek et al., 2007 and Sukeova et al., 2007). The cross-correlation properties of the L2C are excellent as the CM and CL codes are 10 times and 75 times longer, respectively, than the C/A. Therefore, the L2C is superior to C/A in signal tracking and recovery performance (Cho et al., 2004). As the CL code does not include navigational messages, its acquisition performance is higher than the other codes, even in harsh operational environments, for instance, indoors and under bushes (Fontana et al., 2001).

Traditional geodetic-grade GPS receivers adopting a codeless or semi-codeless tracking technique for the second carrier-phase deliver relatively low strength in the corresponding signal. In contrast, tracking of L2C, a GPS modernised signal, results in reducing the occurrence of cycle slips and maintaining the continuity of tracking as L2 carrier-phase are acquired in full strength; however, the time to acquire the first data takes a bit longer compared to that of C/A due to the code length (Lim et al., 2006 and Song et al., 2011).

## 3. Data and Quality Measures

### *3.1 Testing Data Sets*

To assess the overall quality of the GPS L2C signal, the authors secured PR and CPH data sets for various conditions of the receiver types and dynamics and multipath environments (e.g., see Table 3). The observation sets can be classified according to the receiver types into those at permanent stations (i.e., CORS – continuously operating reference stations) and those observed by high-performance and cost-effective receivers at temporary stations. In the latter case, GPS data were acquired by sub-classifying the receiver dynamics into static and kinematic mode and the multipath environments into benign and adverse. As shown in Figure 1, 'observation set I (hereafter SET I)' was measured by CORSs of international GNSS services (IGS) and the national geographic information institute of Korea (NGII). To compare the signal quality between eight receiver models—Javad TRE_3, Leica GR30 and GR50, Septentrio PolaRx5 and PolaRx5TR, Topcon NET-G3A, and Trimble NETR9 and ALLOY, we obtained observations from a total of 24 stations, three for each model. The observations are for a 24-h duration in 1-s intervals, and the data for NGII were acquired on July 5, 2021, whereas those from IGS were acquired on July 22–28, 2021.

'Observation set II (hereafter SET II)' was acquired by installing temporary stations (e.g., see the left photograph in Figure 2) and using Javad Alpha and Leica GS07 (i.e., geodetic-grade receivers), and U-blox ZED-F9P board (i.e., a cost-effective device). The measurements were obtained for 4-h in 1-s intervals in a benign multipath environment. Additionally, to identify the noise characteristics that could not be analysed using the CORS data, zero-baselines were configured by two identical receivers for Alpha and ZED-F9P to acquire signals. For 'observation set III (hereafter SET III)', GPS data were made in a relatively adverse multipath environment (e.g., see right photograph in Figure 2); other observation conditions were identical to those of SET II. The dataset was obtained on the day after the campaign for SET II, and to eliminate the effect of the geometry of SVs in the quality assessment of observations acquired on different days, the

observation time on the following day was set to be 4 minutes earlier than that on the previous day, considering the orbital cycle of the satellites. For 'observation set IV (i.e., hereafter SET IV)', GPS data were collected for 1-h while moving along the path shown in Figure 3 after installing GPS antennas and receivers in a vehicle.

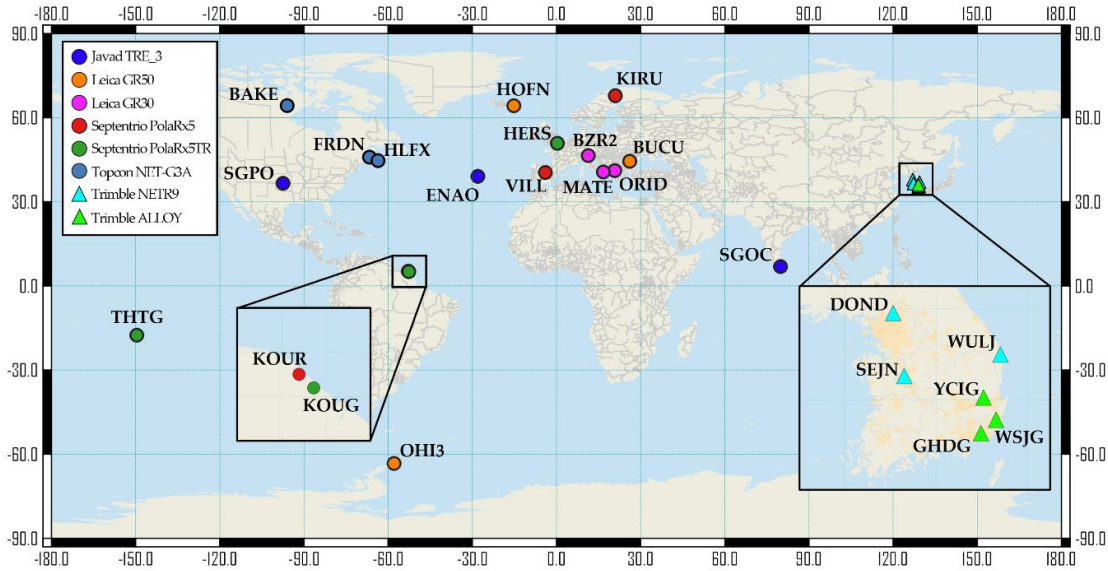


Figure 1: Distribution of the stations acquiring SET I

Figure 2: Equipment setups for obtaining SETs II and III: the left photo shows benign environment while that of right is observation under harsh environment

Table 3: Overview of GPS observations analysed in this study

| Observation sets | Receiver Types | Dynamics | Multipath environme | Remark |
|---|---|---|---|---|

| | | | nt | |
|---|---|---|---|---|
| I | Geodetic-grade | Static | Benign | CORS |
| II | Geodetic and cost-effective models | | | - |
| III | | | Adverse | - |
| IV | | Kinematic | - | Driving along the main street of a city center |

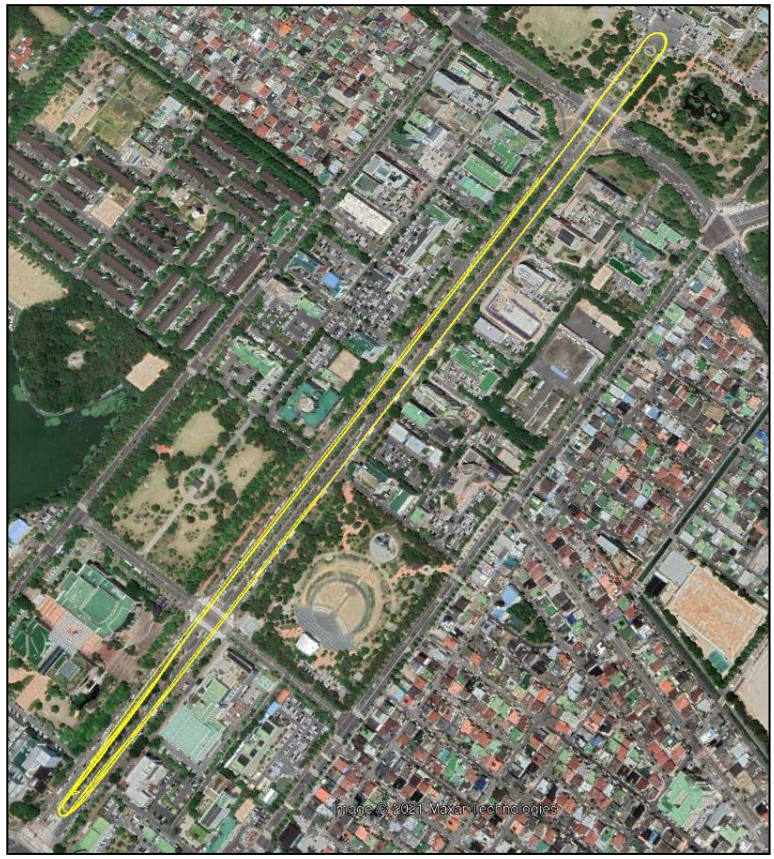


Figure 3: Vehicle trajectory during the field experiment for SET IV

Note that the driving speed was kept constant at about 40km/hr during the data collection, except for a vehicle's maneuvering according to traffic and road geometric conditions (Table 3).

As mentioned in the previous section, since the GPS L2C signal consists of two codes, the receiver can acquire the PR and CPH by tracking CM and CL codes, respectively or simultaneously. The receivers used in this study were products of five manufacturers: data were acquired from the two codes of L2C for the products of Trimble and Javad, from CL for Septentrio, Topcon, and U-blox, and from CM for Leica.

*3.2 Quality Measures*

The measures used in the study to assess the signal quality of the GPS L2C together with C/A and P2(Y) are: (a) signal-to-noise ratio (SNR); (b) data acquisition rate; (c) PR multipath; (d) noise level. The numerical values characterising the quality indices were determined by each type of receiver of the observation sets (e.g., SET I to IV). The method of determining the representative value of each quality measure is described below. SNR is the ratio of the amplitude of the recovered carrier signal to the noise and is an indicator of the signal's strength and received signal quality (Bilich et al., 2004, De Agostino et al., 2008 and Steigenberger et al., 2020). To characterise the SNR of each receiver, the mean and standard deviation of the SNR for each SV were calculated and then averaged for all the satellites. The data acquisition rate is an index that compares the number of L2C data with legacy signals. For the ranging code, it was calculated as the ratio of the number of L2C and P2(Y) data, respectively, to the number of acquired C/A data; for the carrier-phase, it was calculated as the ratio of

the L2 acquisitions for L2C and P2(Y), respectively, to L1.

The magnitude of the PR multipath is computed by substituting the dual-frequency data into Equations 1 & 2 (al-Fanek et al., 2007 and Sukeova et al., 2007). The value representing the multipath Here, to remove the integer ambiguity term of the carrier-phase data, the nearest integer values were subtracted from the double-differenced measurements (Park and Kee, 2006). Note that the noise of single SV's measurements is characterised by a standard deviation of the values computed by the aforementioned method.

$$\Delta M_1 + \varepsilon_1 = \rho_{code,1} - \frac{f_1^2+f_2^2}{f_1^2-f_2^2}\rho_{phase,1} + \frac{2f_2^2}{f_1^2-f_2^2}\rho_{phase,2} = \rho_{code,1} - 4.0915\rho_{phase,1} + 3.0915\rho_{phase,2}$$

Equation 1

$$\Delta M_2 + \varepsilon_2 = \rho_{code,2} - \frac{2f_1^2}{f_1^2-f_2^2}\rho_{phase,1} + \frac{f_1^2+f_2^2}{f_1^2-f_2^2}\rho_{phase,2} = \rho_{code,2} - 5.0915\rho_{phase,1} + 4.0915\rho_{phase,2}$$

Equation 2

where $\boldsymbol{\Delta M_i}$ and $\boldsymbol{\varepsilon_i}$ represent the PR multipath and noise, respectively; $\boldsymbol{\rho_{code,i}}$ and $\boldsymbol{\rho_{phase,i}}$ are the PR and CPH measurements (m); and $\boldsymbol{f_i}$ is the frequency. The subscript $\boldsymbol{i}$ is classified into L1 (1575.42 MHz) and L2 (1226.60 MHz) according to the carrier band.

properties of each receiver was determined by the standard deviation of the multipath for each SV tracked and then averaging it for a total number of satellites. Noise can be given by double-differencing PR and CPH measurements of the so-called zero-baselines (Quan et al., 2016).

## 4. Results and Discussions

### *4.1 Analysis of Data Obtained at CORSs*

The SET I has been examined to address the impact of geodetic receivers on the quality of GPS L2C signals and measurements. Figure 4 shows the SNRs fluctuation of the modernised PRN05 and legacy PRN19 at DOND station in Korea. The left graph in the figure presents that L2C signal strengths are not much diverse from the first civilian code (i.e., C/A) but different in pattern from the encrypted military code (i.e., P2(Y)). It is also of interest to compare the P2(Y) SNR variation of the legacy and modernised SV. For instance, the SNR values of the legacy P2(Y) are smaller than the C/A at all satellite elevation, whereas those of the modernised SV is most prominent among the signals if the elevation angle is higher than about 50°. The reason that the SNR of P2(Y) is smaller than those of other signals should be that the signal is acquired in a codeless or semi-codeless tracking technique (Hofmann-Wellenhof et al., 2001 and Grewal et al., 2020). In contrast, the modernised SVs are equipped with a high-strength P(Y) signal transmitter and emit strong signals in certain regions by receiving commands from the control segment to increase the resistance to jamming. Therefore, the signal strength of P2(Y) is significantly enhanced at certain elevation angles (Esenbuğa and Hauschild, 2020 and Steigenberger et al., 2020).

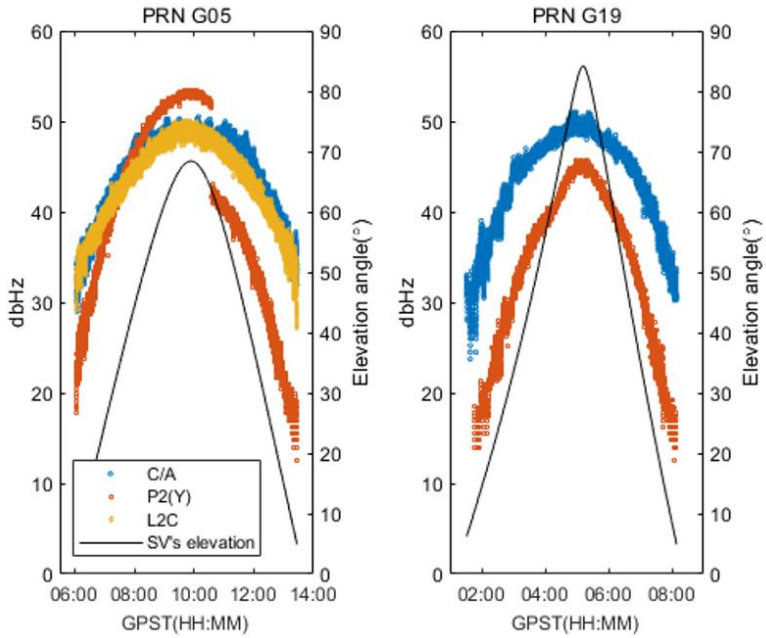


Figure 4: Signal-to-noise ratio on GPS ranging signals with the variation of satellite elevation at DOND station in Korea: the left graph presents the modernised SV (i.e., PRN 05) while that of the right is the legacy PRN 19

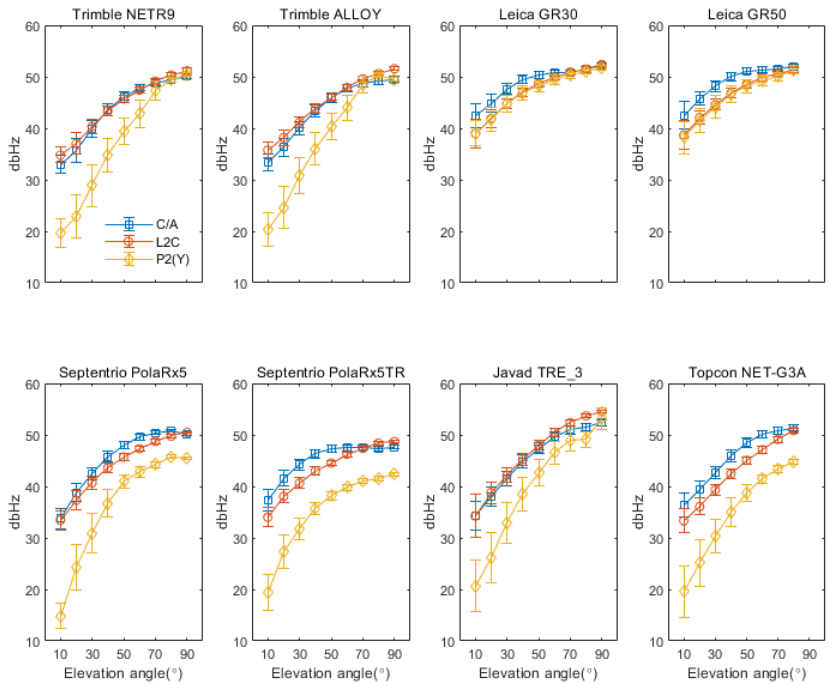


Figure 5: Signal-to-noise ratio on GPS ranging signals of geodetic grade receivers

Table 4: Data acquisition rates of SET I (unit: %)

| Observations | Pseudo-ranges | Carrier-phases |
|---|---|---|

| Receivers | L2C | P2(Y) | L2C | P2(Y) |
|---|---|---|---|---|
| Javad TRE_3 | 100.12 | 97.98 | 100.12 | 97.98 |
| Leica GR50 | 99.87 | 99.91 | 99.95 | 99.95 |
| Leica GR30 | 99.86 | 99.86 | 100.05 | 99.90 |
| Septentrio PolaRx5 | 100.14 | 99.96 | 100.54 | 99.93 |
| Septentrio PolaRx5TR | 100.00 | 100.00 | 99.28 | 99.57 |
| Topcon NET-G3A | 99.78 | 99.28 | 99.78 | 99.28 |
| Trimble NetR9 | 99.62 | 99.13 | 100.57 | 99.31 |
| Trimble ALLOY | 99.88 | 99.68 | 100.31 | 99.74 |

Figure 5 depicts the mean and standard deviation of the SNRs for an elevation angle section of 10° for all the receiver models considered in this study, presenting that the characteristics of the three signal strengths are resembling. However, the SNRs of the two civilian codes obtained by Trimble and Javad are almost identical, but the L2C strengths of Leica, Septentrio and Topcon are slightly lower than those of C/A. This may be related to L2C tracking techniques adopted by the manufacturers; for example, Trimble and Javad trace multiplexed CM and CL (i.e., CM+CL) while the other manufacturers acquire either CM or CL. On the other hand, the figure shows that the P2(Y) SNRs are smaller than the civilian signals in all receiver models except for the Leica. Furthermore, it can be observed from the graphs that the lower elevations are, the more significant gaps in the SNR values of the civilian and military signals become, and vice versa. On the other hand, Figure 6 shows the means and standard deviations of the SNR computed to three CORSs equipped with the same receivers to present the manufacture dependent properties of signal strength of the GPS ranging codes. Overall, the results indicate that L2C strength is equivalent to or slightly lower than C/A but higher than P2(Y).

Table 4 summarises the averaged data acquisition rates of each receiver type for SET I. The PR and CPH rates of L2C are 99% or higher for each receiver model; the latter, especially, exceeded 100% in most models, i.e., the acquisition is higher than C/A observations. The comparison of the L2C and P2(Y) in the table reveals that the former's rates are higher in most receiver models despite the marginal differences (Table 4). As an example of the typical multipath pattern, the multipath of PRN05 at DOND is shown in Figure 7, along with the elevation angle of the SV. As well known (e.g., al-Fanek et al., 2007, Sukeova et al., 2007 and De Agostino et al., 2008), the magnitude of the multipath is coupled with an elevation angle as seen in the figure; namely, the lower angle is, the stronger the error becomes. To compare the multipath with respect to elevation angles and receiver types, the multipath values in angle intervals of 10° for each receiver are distinguished and the averaged values for each interval are depicted in Figure 8. L2C multipath of Trimble receivers becomes smaller than C/A as the elevation angle increases; however, the L2C multipath of Javad and Topcon is more severer than C/A at all elevation angles. Furthermore, it is a bit hard from the results to characterise the multipath property of the other receivers.

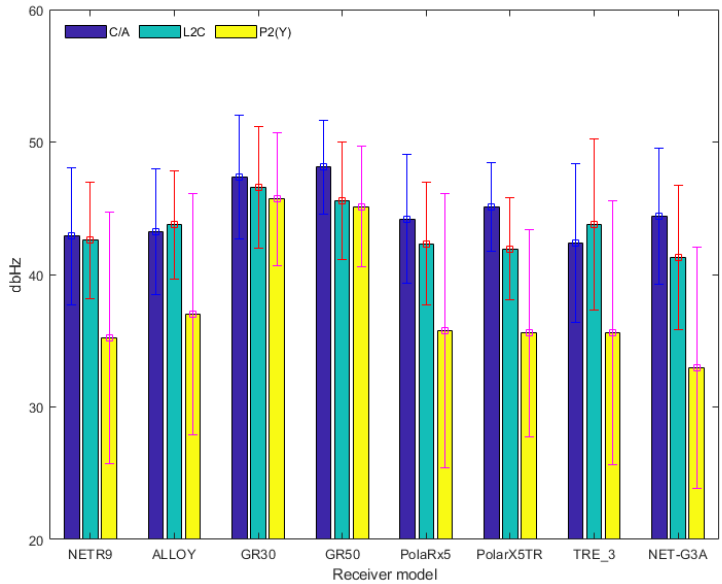


Figure 6: Averages and standard deviations of SNR on GPS ranging signals of geodetic grade receivers captured from SET I

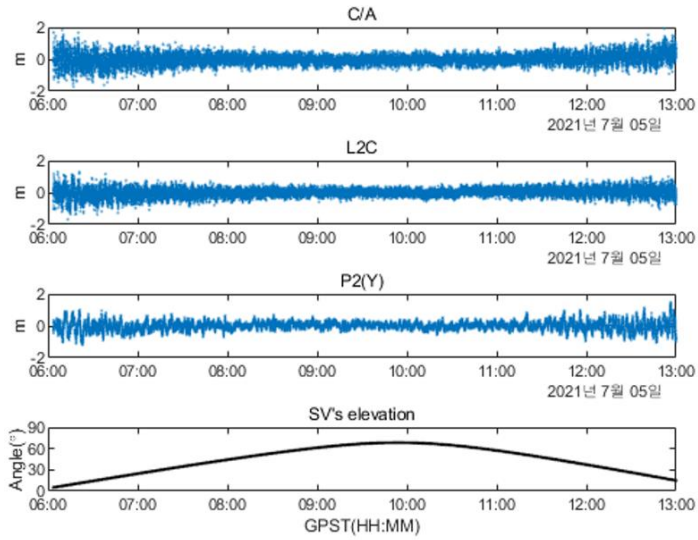


Figure 7: PR multipath of PRN 05 tracked at DOND station in Korea

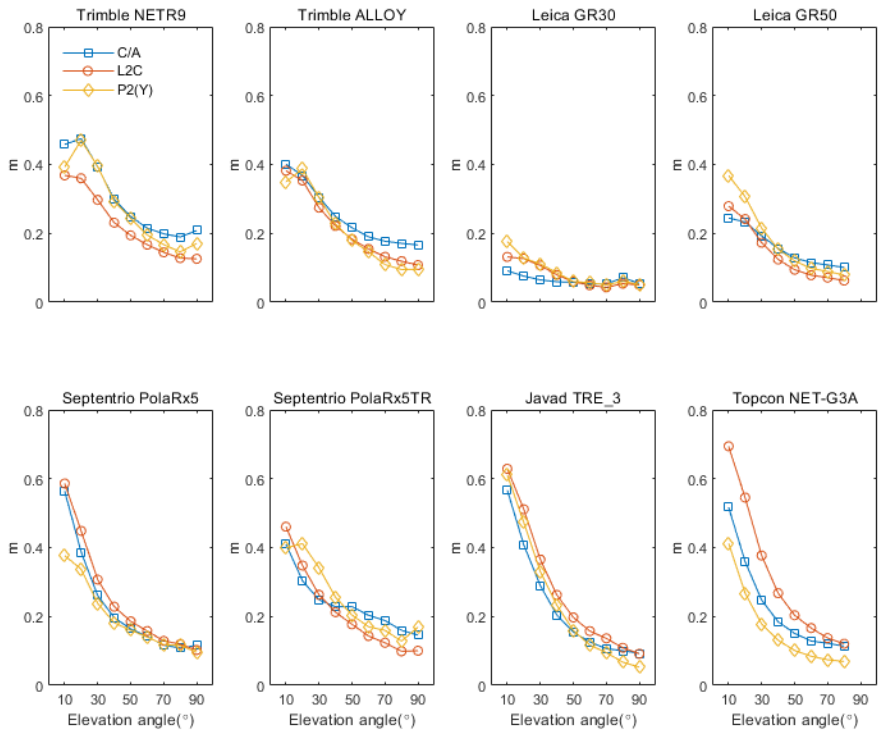


Figure 8: PR multipath of geodetic grade receivers computed from SET I

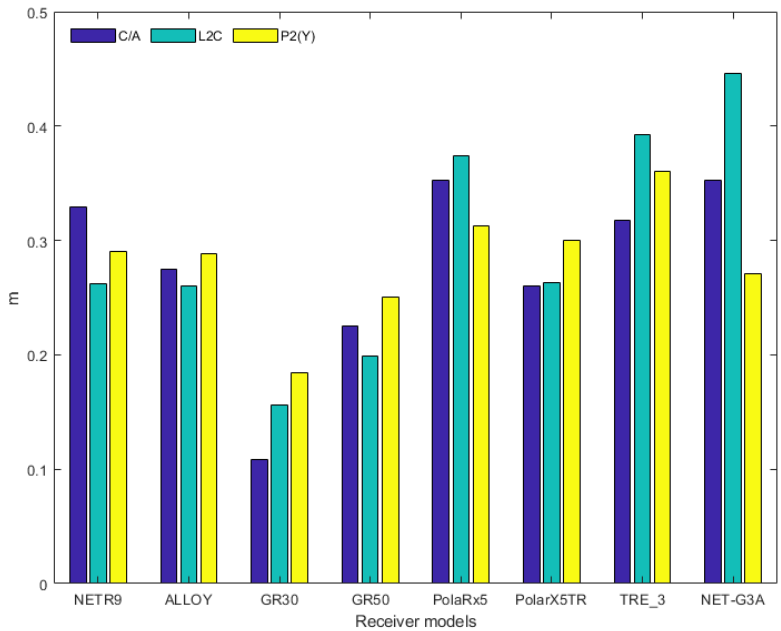


Figure 9: Averages of PR multipath of the geodetic grade receivers

For the overall comparison of L2C multipath with C/A and P2(Y), the computed multipath at three CORSs for each receiver type has been averaged and shown in Figure 9. Nevertheless, a unique pattern of the multipath among the codes cannot be observed from the results, but it seems to be more dependent on receivers as a slightly different tracking technique along with a multipath mitigation algorithm would be implemented.

*4.2 Comparison of Observations Made at the Temporary Station by Experiment*

To examine the L2C signal quality based on the grade of GPS receivers and the observation environment, the quality indicators of observation SET II and III have been analysed. The noise level is also evaluated along with the three quality measures based on double-differencing the zero-baseline measurements of Javad Alpha and U-blox ZED-F9P device.

As presented in Figure 10, the means and standard deviations of the SNR for SET II and III have been computed to examine the features of the signal strengths obtained by the different grades of receivers under a benign and harsh multipath environment. The left graph of Figure 10 presents that the SNR for L2C of the two geodetic-grade receivers was higher than that of C/A, whereas ZED-F9P—a cost-effective receiver—showed the opposite result. The SNR trend of Alpha was the same as that of TRE_3, a receiver of the same manufacturer, in Figure 6. On the other hand, the relative trends between L2C and C/A of Leica GS07 diverge from those of GR30 and GR50 of the same manufacturer in Figure 6; the P2(Y) signal strength is higher than those of the others, at similar levels to those of C/A and L2C. The trends for the two signal strengths of ZED-F9P are similar to the results of the Septentrio, and Topcon receivers as the receivers of the three manufacturers acquire the pseudo-ranges from the CL code. Comparing the SNR of SET III with the results of SET II reveals that the relative trends between the three ranging signals are almost the same. Table 5 summarises the data acquisition rates for SET II and III. In the results of SET II, the L2C and P2(Y) pseudo-range and carrier-phase acquisition rates of each receiver are greater than or equal to 99%, indicating no significant difference in the number of observed data for the three signals.

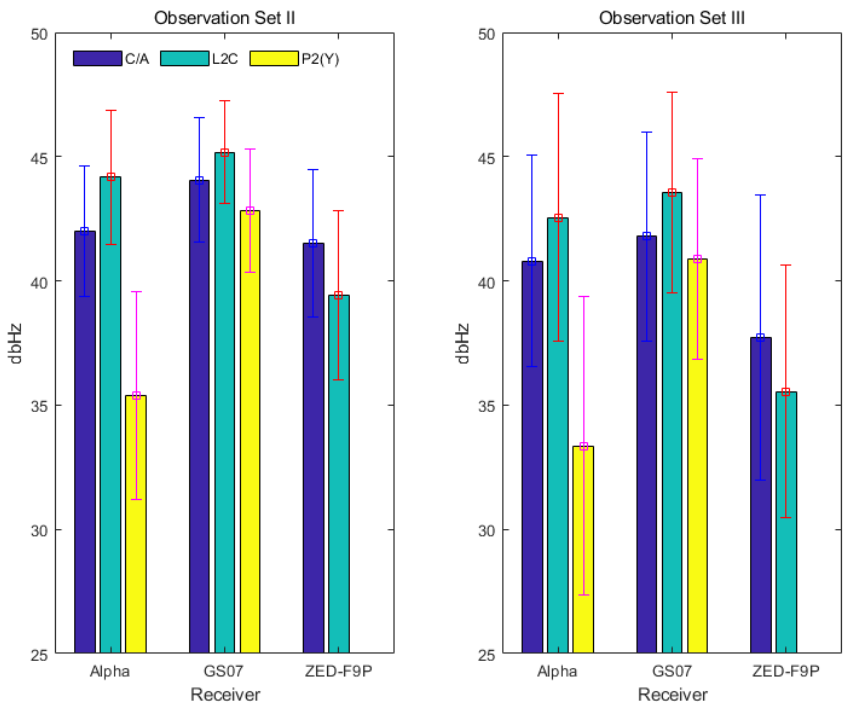


Figure 10: Averages and standard deviations of SNR on the ranging signals of SETs II and III

Table 5: Data acquisition rates of SETs II and III (unit: %)

| SETs | II | | | | III | | | |
|---|---|---|---|---|---|---|---|---|
| Measurements / Receivers | Pseudo-range | | Carrier-phase | | Pseudo-range | | Carrier-phase | |
| | L2C | P2(Y) | L2C | P2(Y) | L2C | P2(Y) | L2C | P2(Y) |
| Javad Alpha | 99.99 | 99.58 | 99.99 | 99.58 | 99.77 | 94.56 | 99.77 | 94.56 |
| Leica GS07 | 99.94 | 99.86 | 100.06 | 99.90 | 98.04 | 97.27 | 99.36 | 98.04 |
| U-blox ZED-F9P | 100.73 | - | 99.69 | - | 103.32 | - | 94.77 | - |

In the case of SET III (e.g., adverse multipath environment), the acquisition rates of the L2C codes and phases of the high-performance receivers were between 98.04 and 99.77%. On the other hand, the P2(Y) rate decreased overall, showing 94.56% for Alpha and 97–98% for GS07. These results suggest that acquiring L2C instead of P2(Y) by using geodetic-grade receivers effectively maintains the continuity of GPS positioning. In the results of the low-cost receivers, the number of L2C pseudo-range acquisitions was more significant than that of C/A, but the carrier-phase acquisition decreased to 94.77%.

For comparing the multipath properties of the SET II and III, the averaged values are depicted in Figure 11. The results of the benign condition (i.e., the left graph) show that the L2C multipath is more significant than the C/A regardless of the type of tracking codes. Note that Leica, u-Blox and Javad receiver acquire the PR by tracking CM, CL, and multiplexing the two codes, respectively. In the comparison of the results of the two high-performance receivers with those of the same manufacturers among CORS, the size and tendency of the multipath of GS07 are similar to that of the GR30 in figure 9; Alpha shows a resembling trend to TRE_3, but its size is 20 cm larger in all three signals because the multipath mitigation algorithm option is not applied to the Alpha receiver used in the experiment. In the results of SET III acquired in a harsh operational environment, Alpha's C/A and L2C multipath maintains the relative magnitude as shown in the left graph in Figure 11 with increased size, whereas in GS07 and ZED-F9P, the multipath of C/A is comparable to or slightly larger than that of L2C. The magnitude of multipath of ZED-F9P increases 1.5 times as the operating condition becomes adverse. Unlike the other two receivers, this can be interpreted as indicating that ZED-F9P is relatively more sensitive to the observational environment than Alpha and GS07. Despite obtaining the observation at the same location with three receivers, it is possible to observe differences in the absolute size and relative tendency of multipath among each signal owing to the difference in the multipath mitigation and signal tracking algorithm implemented in each receiver. The commonality in the results of PR multipath of high-performance receivers is that as the observational environment becomes harsh, the magnitude of the multipath of P2(Y) increases compared to that of the other two signals. Therefore, the use of L2C instead of P2(Y) would be able to improve slightly the positioning performance such as ambiguity resolution, especially under an adverse observational environment. When tracking SV's signals with a cost-efficient receiver ZED-F9P, the positioning accuracy may decrease due to a considerable increase in the multipath as the observation condition becomes harsh.

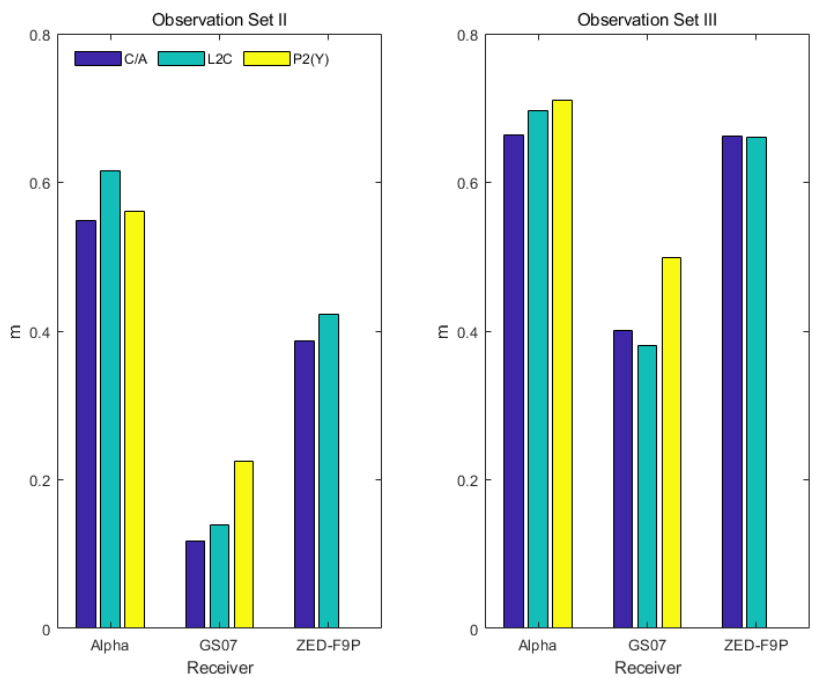


Figure 11: Averages of PR multipath of SETs II and III

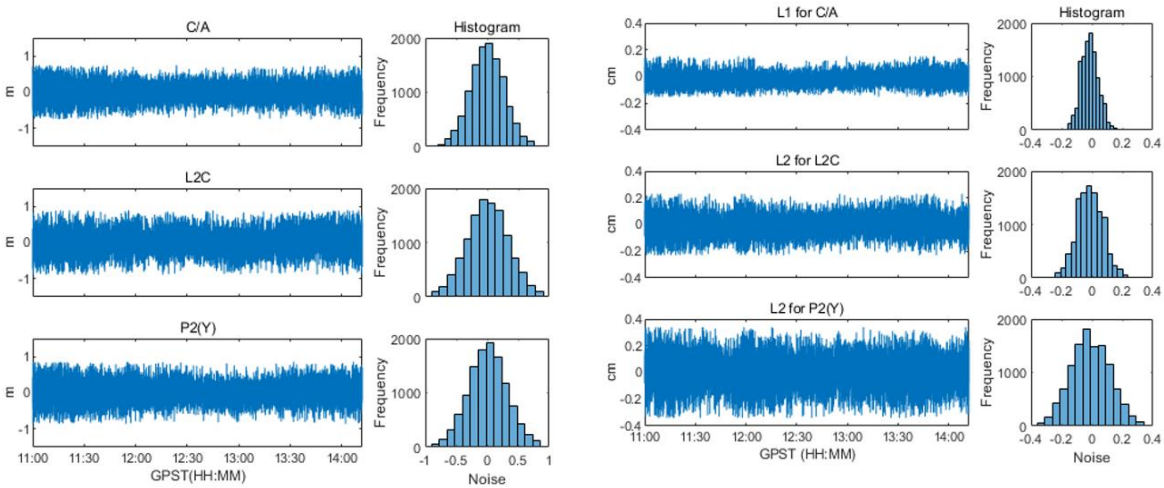


Figure 12; Time-series and histograms of GPS measurements noise: the left graphs depict the PR of PRN 29 obtained by an Alpha receiver under the benign operational environment (i.e., SET II) while those of the right show the CPH

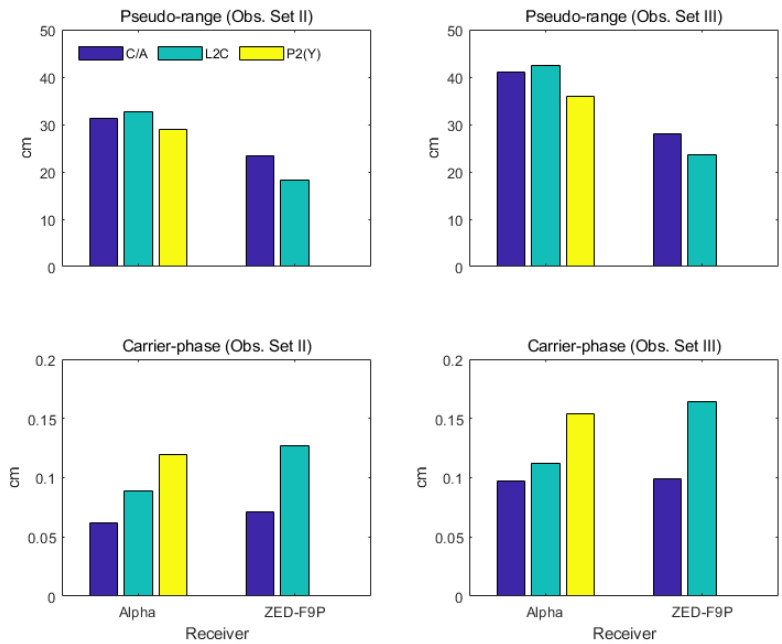


Figure 13: Averages of noise standard deviations: the left graphs are results of SET II, whereas those of the right are from SET III

Figure 12 demonstrates an example of the noise of the PR and CPH with their histograms for the observations acquired from PRN 29 using Alpha in SET II. In Figure 12, the noises of the three PRs are similar, and as for the CPH, L1 having a shorter wavelength is the least among the three signals, and L2 extracted from L2C is smaller than that of P2(Y). The histograms for these noise values have shapes almost identical to a normal distribution, implying that the noise was calculated appropriately according to the method introduced in the Quality measures section. Figure 13 shows the average values of the PR and CPH noises of Alpha and ZED-F9P that received signals from SVs by constructing the zero-baseline in SETs II and III. In the results of SET II, the PR noise for L2C of Alpha is slightly larger than that of C/A, but the difference is insignificant. The reason for this result would be that the chip rate of L2C obtained with Alpha is identical to that of C/A owing to Alpha's PR of L2C is derived from multiplexed two codes (i.e., CM + CL).

The two PR noises of ZED-F9P show the opposite trend, and the difference is relatively distinct. Because the L2C PR of ZED-F9P was acquired from the CL code, which is longer than the C/A code, the noise is expected to be greater than that of the legacy signal, but the contrastive result is observed, likely due to the effect of the data acquisition algorithm of the receiver. The P2(Y) PR noise of Alpha is the smallest among those of the three signals, but the difference is slight. In the carrier-phase noises acquired under a benign operational environment, the noise for L1 with a short wavelength is smaller than L2, as shown in Figure 12 in both receivers. In the result of Alpha, the L2 noise corresponding to L2C is less than that of P2(Y). As the operating environment become adverse, the PR and CPH noise levels are increased, but the relative magnitude of each measurement is maintained. Based on the comparisons of each signal's noise, it will be rational to obtain L2C, which has a smaller noise level, instead of P2(Y) in the CPH-based positioning applications that typically use high-performance receivers. The effect will be even more significant in a harsh observational environment. When ZED-F9P, a cost-effective receiver, is utilised in the PR-based positioning applications, the usage of L2C, which has a trim noise level, will be favourable for improving the positioning accuracy.

*4.3 Analysis of Kinematic Data*

To evaluate the impact of moving the receiver on the quality of the L2C signal, SET IV acquired from receivers and antennas set up on a driving vehicle has been analysed by using the four quality measures aforementioned in session 2. Figure 14 presents the SNR and elevation angle for three signals of satellite PRN26 tracked by Alpha, and it includes the signal strength of the data observed in the stopped vehicle for 30 min before moving the receiver. In Figure 14, the considerable change in SNR is observable as the hardware moving. Therefore, the average and standard deviation of the four quality measures were computed with only the data acquired when the receiver was moving. Figure 15 shows the mean and standard deviation of the signal strengths for SET IV. In the figure, the relative tendency of SNR in three signals for all receivers is almost identical as shown in the results of SETs II and III. The strength of the signals received by GS07 and ZED-F9P are similar in size to that of SET II, but the size for Alpha's ones decreases significantly because the dynamics setting of the receiver was changed from static to dynamic for the experiment in the moving environment. Figure 16 shows the data acquisition rates for SET IV. The L2C PR and CPH acquisition rates of the three receivers are over 98%, showing no significant difference from the number of C/A acquisitions. Especially, the PR acquisition rate of ZED-F9P is approximately 102%, and the CPH acquisition rate of GS07 is approximately 106%, indicating that a significantly larger number of data was acquired than that of C/A.

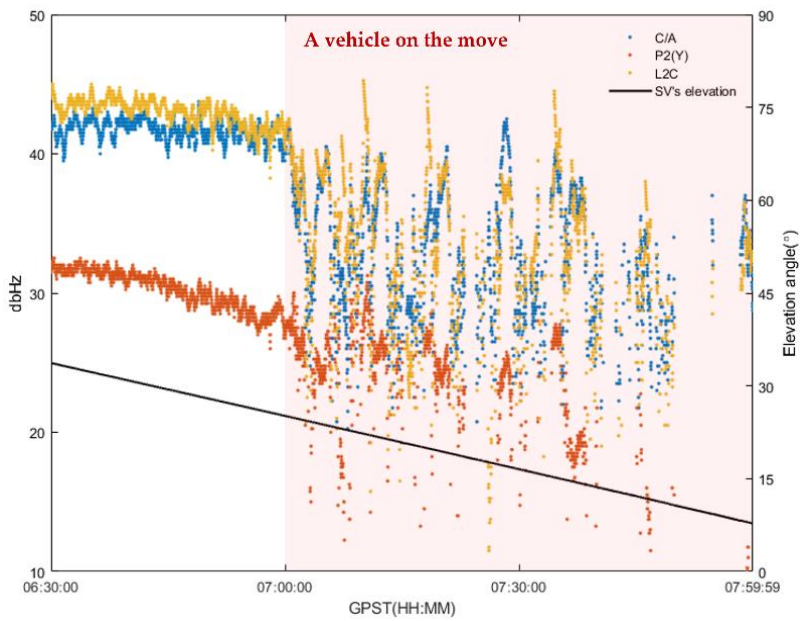


Figure 14: Signal-to-noise ratio on GPS ranging signals of PRN 26 in the kinematic test

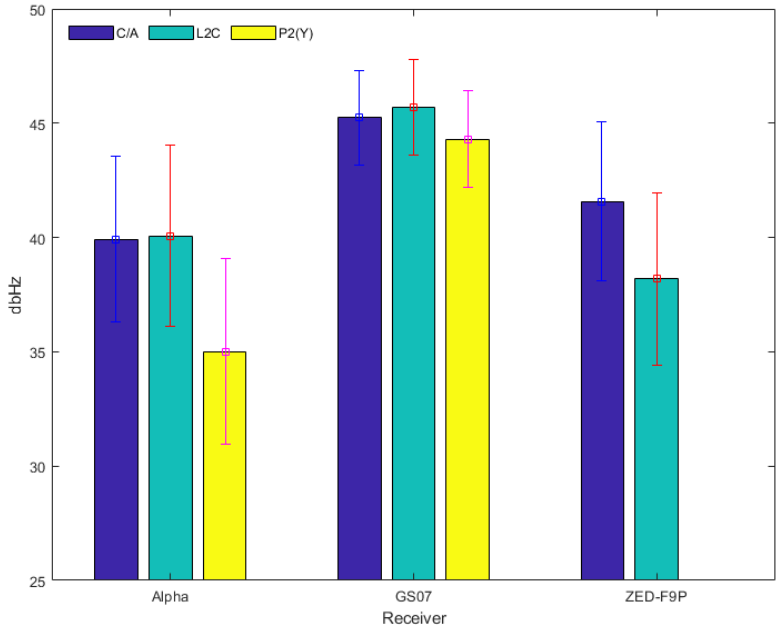


Figure 15: Averages and standard deviations of signal-to-noise ratios on ranging signals of the kinematic test

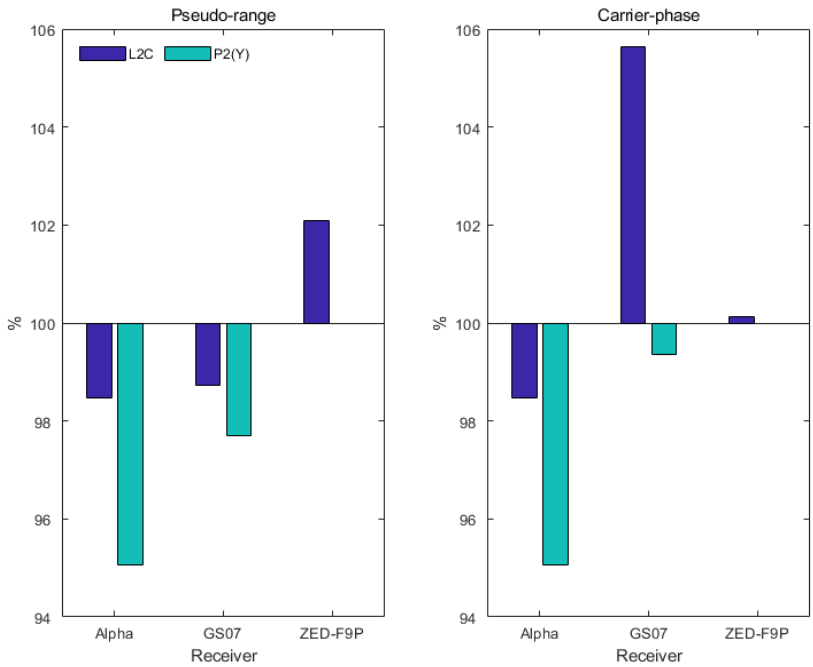


Figure 16: Averages of data acquisition rates of ranging signals of the kinematic test

The PR and CPH acquisition rates of P2(Y) decrease remarkably to 95% for the Alpha receiver. Those for GS07 are 98%, but they are still lower than those of L2C. Therefore, receiving L2C signal in an environment where the equipment is moving will be effective in acquiring data and improving the continuity of positioning. To analyse the impact of the hardware's movement on the PR multipath, the mean multipath for each receiver for SET IV (Figure 17) has been calculated. The L2C multipath of Alpha and ZED-F9P is larger than that of C/A, whereas that of GS07 shows the opposite result. Because the geometry of SVs for SET IV is different from those of SETs II and III, it is difficult to compare the absolute size among them, but the relative tendency for the three PRs is confirmed in the earlier result (Figure 11).

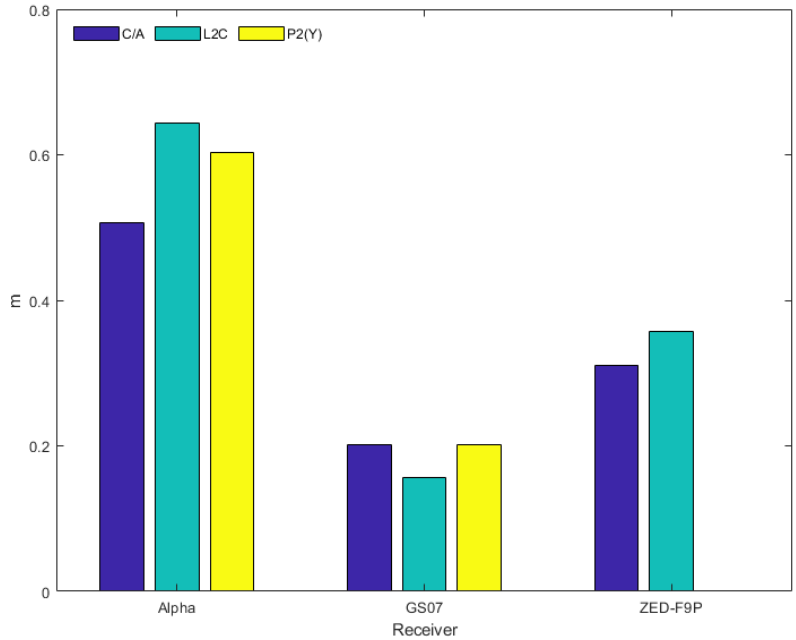


Figure 17: Averages of PR multipath of the kinematic test

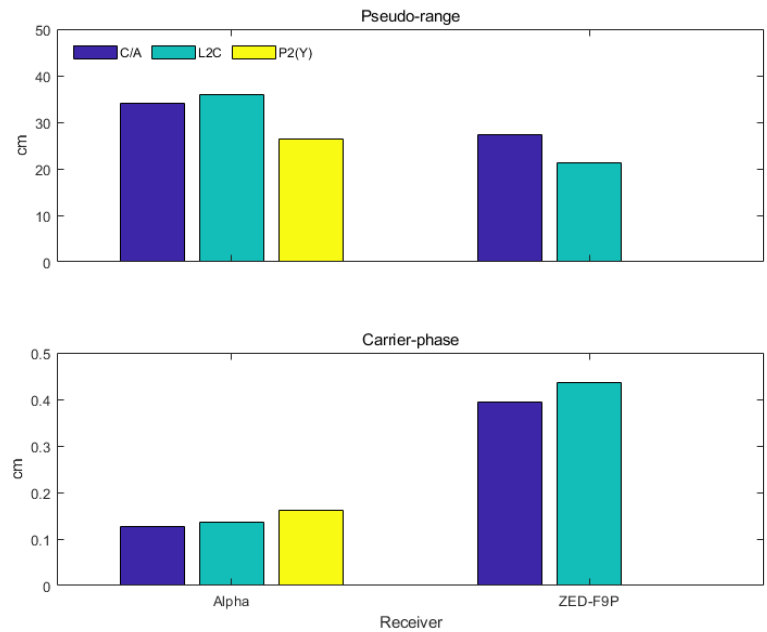


Figure 18: Averages of noise standard deviations of the kinematic test

The analysis result of the PR multipath in the kinematic experiment shows that the movement of hardware does not have much impact on the relative trend of each signal in this measure. Therefore, the use of L2C under a kinematic environment wouldn't have a significant effect on the positioning performance in terms of accuracy. Figure 18 presents the averaged noise level of the data acquired by Alpha and ZED-F9P in SET IV. The relative magnitude for the noise in three signals of PR and CPH obtained by the two receivers, respectively, is the same as that examined in SETs II and III. The noise level is slightly higher compared to that of the result in the benign environment; particularly, the CPH noise level of ZED-F9P is increased around five times.

Acquiring L2C instead of P2(Y) in CPH-based positioning that usually uses a high-end receiver is not expected to have a large impact on the positioning accuracy improvement in a kinematic environment; however, it can improve signal tracking and continuity of the solution and thus it will be desirable to receive L2C signal. In PR-based positioning with a low-cost receiver, the additional usage of L2C, which has a low noise level, would be able to improve the accuracy of the solution.

## 5. Concluding Remarks

In this study, the characteristics of L2C GPS signals and measurements have been intensively assessed compared to those of C/A and P2(Y) under various observation conditions, such as GPS receiver models, grades, dynamics, and operational environments. The findings from the experiments and the analyses can be summarised below:

(a) The strengths and acquisition rates of the GPS L2C and C/A code are generally equivariant, but those of the P2(Y) are much smaller than the others, especially under a harsh multipath environment. In addition, relative differences between the two quality measures among the three signals depend upon receiver manufacturers, observational condition (e.g., multipath environment and dynamics), and type of L2C codes used for extracting measurements (i.e., CM and CL). It is fascinating to observe that the SNR of ZED-F9P obtained L2C is more significant than C/A.

(b) The three GPS codes' absolute and relative multipath magnitude heavily rely upon a receiver model as they employ different tracking and multipath mitigation techniques; hence, the results cannot prove which code signal is robust to the multipath error. In addition, although the multipath increases under adverse operational conditions, the P2(Y) increment is relatively more significant.

(c) The noise of L2C-extracted CPH is larger than that of C/A, as expected from the wavelength. However, the L2C CPH noise is more diminutive than P2(Y) because of its tracking efficiency. On the other hand, the PR noise acquired from the signals depends upon a receiver model.

(d) Comprehensively considering all the results of this study, it is possible to conclude that the quality of GPS L2C signal and measurements is equivalent to C/A and better than P2(Y), particularly in terms of the signal strength and data acquisition rate, and noise level; and signal tracking the performance of a cost-effective GPS chipset is almost in a class with a high-end receiver.

Finally, it is crucial to note that the results of this study have been drawn from GPS signals and measurements obtained under a specific experimental condition in this study; hence they would be slightly varied if a different signal tracking situation is applied. Nevertheless, it is believed that the paper contributes a practical understanding of the modernised GPS signal characteristics to researchers who have been developing a novel positioning algorithm based on L2C measurements.

## References


al-Fanek, O., Skone, S., Lachapeele, G. and Fenton, P., 2007, Evaluation of L2C Observation and Limitations. *in Proceedings of the 20th International Technical Meeting of the Satellite Division of the Institute of Navigation (ION GNSS 2007)*, 2510-2518.

Bilich, A., Larson, K. M. and Axelrad, P., 2004, Observations of Signal-to-Noise Ratios (SNR) at Geodetic GPS Site CASA: Implications for Phase Multipath. *Proceedings of the Centre for European Geodynamics and Seismology*, 77-83.

Cho, D. J., Park, C. and Lee, S. J., 2004, An Assisted GPS Acquisition Method Using L2 Civil Signal in Weak Signal Environment. *Journal of Global Positioning Systems*, Vol. 3, 25-31.

De Agostino, M., Piras, M. and PorPorato, C., 2008, The New L2C GPS Code: Signal and Positioning Quality Analysis. *Proceedings of the 21st International Technical Meeting of the Satellite Division of the Institute of Navigation (ION GNSS 2008)*, 1649-1657.

Esenbuğa, O. G. and Hauschild, A., 2020, Impact of Flex Power on GPS block IIF differential code biases. *GPS Solutions*, Vol. 24, 1-9. doi: https://doi.org/10.1007/s10291-020-00996-x.

Esper, M., Chao, E. L. and Wolf, C. F., 2020, *2019 Federal Radionavigation Plan*, No. DOT-VNTSC-OST-R-15-01. United States. Dept. of Defense.

Fontana, R. D., Cheung, W., Novak, P. M. and Stansell, T. A., 2001, The New L2 Civil Signal. *Proceedings of the 14th International Technical Meeting of the Satellite Division of The Institute of Navigation (ION GPS 2001)*, 617-631.

Grewal, M. S., Andrews, A. P. and Bartone, C. G., 2020, *Global Navigation Satellite Systems, Inertial Navigation, and Integration*, 4th edition, (John Wiley & Sons).

Hofmann-Wellenhof, B., Lichtenegger, H. and Collins, J., 2001, *Global Positioning System: Theory and Practice*, 5th revised edition, (New York: Springer-Verlag/Wien).

Jia, Z., Chen, Z., Yu, P., Lin, M. and Liu, X., 2016, Comparison of the Multipath Effect between Trimble R7 and Topcon NET-G3A. *2016 IEEE International Geoscience and Remote Sensing Symposium (IGARSS)*. 7465-7468. doi: 10.1109/IGARSS.2016.7730947.

Lim, D. W., Moon, S. W., Park, C. and Lee, S. J. 2006, The Fast Signal Acquisition Scheme for a GPS L1/L2C Correlator. *Journal of Institute of Control, Robotics and Systems*, Vol. 12, 765-772. doi: https://doi.org/10.5302/J.ICROS.2-006.12.8.765.

National Oceanic and Atmospheric Administration (NOAA), 2021a, GPS Modernization [online], https://www.gps.gov/systems/gps/modernization / (Date accessed: 11.19.2021).

National Oceanic and Atmospheric Administration (NOAA), 2021b. New Civil Signals [online], https://www.gps.gov/systems/gps/modernization /civilsignals/ (Date accessed: 11.19.2021).

Park, B. W. and Kee, C. D., 2006, Simplified Noise Modeling of GPS Measurements for a Fast and Reliable Cycle Ambiguity Resolution. *Proceedings of the Institute of Navigation and Port Research Conference*, Vol. 1, 535-540.

Quan, Y., Lau, L., Roberts, G. W. and Meng, X., 2016, Measurement Signal Quality Assessment on All Available and New Signals of Multi-GNSS (GPS, GLONASS, Galileo, BDS, and QZSS) with Real Data. *The Journal of Navigation*, Vol. 69, 313-334. doi: https://doi.org/10.1017/S0373463315000624.

Rizos, C., Higgins, M. B. and Hewitson, S., 2005, New GNSS Developments and their Impact on Survey Service Providers and Surveyors. *Proceedings of SSC2005, Spatial Intelligence, Innovation and Praxis: the national biennial conference of the Spatial Sciences Institute*, 1100-1113.

Simsky, A., Sleewaegen, J. M., Nemry, P. and Hees, J. V. 2006, Signal Performance and Measurement Noise Assessment of the First L2C Signal-in-space. *Proceedings of IEEE/ION PLANS 2006*, 834-839.

Song, S. H., Park, J. W., Park, J. H. and Sung, T. K., 2011, Performance Analysis of Signal Acquisition in L2C Assisted GPS Receivers. *Journal of Institute of Control, Robotics and Systems*, Vol. 17, 61-67. doi: https://doi.org/10-.5302/J.ICROS.2011.17.1.61.

Steigenberger, P., Thoelert, S., Esenbuga, O., Hauschild, A. and Montenbruck, O., 2021, The New Flex Power Mode: from GPS IIR-M and IIF Satellites with Extended Coverage Area. *Inside GNSS* [online], Vol. 15. https://insidegnss.com/the-new-flex-power-mode-from-gps-iir-m-and-iif-satellites-with-extended-coverage-area/ (Date accessed 01.25.2021).

Sukeova, L., Santos, M. C., Langley, R. B., Leandro, R. F., Nnani, O. and Nievinski, F., 2007, GPS L2C Signal Quality Analysis. *Proceedings of the 63rd Annual Meeting of The Institute of Navigation (2007)*, 232-241.

U.S. Coast Guard Navigation Center (NAVCEN), 2022, GPS constellation [online], https://www.navcen.uscg.gov/?Do=constellation Status (Date accessed: 01.28.2022).